

See discussions, stats, and author profiles for this publication at: <https://www.researchgate.net/publication/337509947>

Crop Classification using Multi-spectral and Multitemporal Satellite Imagery with Machine Learning

Conference Paper · September 2019

DOI: 10.23919/SOFTCOM.2019.8903738

CITATIONS

7

READS

1,175

3 authors, including:



[Ivana Nizetic Kosovic](#)

Ericsson, Split, Croatia

24 PUBLICATIONS 73 CITATIONS

[SEE PROFILE](#)



[Toni Mastelic](#)

Ericsson Nikola Tesla, Split, Croatia

20 PUBLICATIONS 360 CITATIONS

[SEE PROFILE](#)

Some of the authors of this publication are also working on these related projects:



Haley Project [View project](#)

Crop Classification using Multi-spectral and Multi-temporal Satellite Imagery with Machine Learning

Lucija Viskovic*
Ericsson Nikola Tesla
Split, Croatia
lucija.viskovic@ericsson.com

Ivana Nizetic Kosovic*
Ericsson Nikola Tesla
Split, Croatia
ivana.nizetic.kosovic@ericsson.com

Toni Mastelic*
Ericsson Nikola Tesla
Split, Croatia
toni.mastelic@ericsson.com

Abstract—Satellite images are highly utilized for detecting land usage, while in recent years a finer-grade crop classification has become important in the context of precision agriculture. However, such classification brings new challenges, which aside from multi-spectral images require exploitation of their multi-temporal properties as well, with pixel-based analysis and larger number of classes. In this paper, we apply several machine learning algorithms on multi-spectral and multi-temporal satellite images and derive crop classification models. The models are applied only on agricultural fields, which can be singled out with the existing land usage classification models. Results show that the random forest outperforms other algorithms with accuracy score of 0.8420 and Kappa score of 0.8157. Detailed analysis of recall and precision scores is given for each crop separately, followed by a comprehensive discussion.

Keywords—remote sensing, satellite images, land usage, crop classification, machine learning

I. INTRODUCTION

Remote sensing refers to information acquisition on a distant target, i.e. an object or a phenomenon, without making a physical contact with the target [2]. It is typically done by using aircrafts or satellites, which collect data reflected from the Earth's surface. The information is acquired through electromagnetic radiation, force fields or acoustic energy using different types of remote sensors that can either be active or passive [4]. Active sensors send a stimulus towards the target and then detect the target's response to that stimulus, while passive remote sensors don't use a stimulus, instead they collect data that is being naturally reflected by the target. That said, with the rapid advance of satellite technology, satellite images have become a relevant source of data as passive remote sensors provided through projects such as Sentinel mission¹, MODIS sensor², ASTER sensor³, Meteosat satellites⁴, and the longest running Landsat⁵.

Satellites provide images in various spectral bands defined by its wavelength and bandwidth. An image of a single band can be represented as a greyscale image, where every pixel of the image represents a value of that band for a specific geographical area. The bands are used for calculating certain indices, such as NDWI (Normalized Difference Water Index) and NDVI (Normalized Difference Vegetation Index), which are utilized for detecting water and vegetation, respectively [5]. Indices are then applied on a pixel basis or on an object/area found in a satellite image, such as agricultural field or urban area [10].

In the last two decades, these indices have been widely used for determining land usage including but not limited to urban areas, agricultural fields and water bodies [1], while in recent years finer-grade classification is being researched, mostly in agriculture targeting crop classification [8][10][16]. However, use of predefined indices has shown lacking due to crop phenology, alteration of crops health and quality during time, as well as soil type [11], which are difficult to differentiate by observing a single index in a single satellite image. That said, use of multi-spectral and multi-temporal satellite images [12] and analyzing them pixel by pixel [10] has proven beneficial in crop classification. However, the challenge remains to properly aggregate multi-temporal images and apply a robust model that is capable of detecting various types of crops.

In this paper, we utilize multi-temporal properties of satellite images by aggregating a sequence of images taken throughout the year and apply machine learning algorithms on 15 different indices of the same area to classify different crops. We use several supervised machine learning algorithms including linear, non-linear and tree-based [3], with ground truth taken from the National Agricultural Statistics Service (NASS) by United States Department of Agriculture [17], a database of agricultural fields and their crops. Total of 12 classification models are built with 10-fold cross validation method, capable of distinguishing 7 different crop types. The models are applied only on agricultural fields, which can be singled out with the existing land usage classifiers.

The best model being the one built with random forest is evaluated on a separate dataset, i.e., completely independent agricultural fields in a different area. The evaluation results show that our methodology with the random forest model achieves best scores for accuracy and Kappa, namely 0.8420 and 0.8157, respectively. More detailed analysis of the evaluation results is provided through confusion matrix that gives recall and precision scores for each crop separately. Finally, a discussion is given on close examination of NASS dataset that is used as the ground truth in our work, which demonstrates issues in their classifications, and potentially better accuracy of our models then given by the evaluation results. That said, contributions of this work are twofold, namely:

- Methodology for analyzing multi-spectral and multi-temporal satellite images for crop classification.
- Successful application of machine learning algorithms within previously proposed methodology.
- Insights on the reliability of ground-truth data and its implications to the model performance.

* These authors have contributed equally and are ordered ascending and alphabetically by their surnames.

¹ <https://sentinels.copernicus.eu/web/sentinel/missions/sentinel-2>

² <https://modis.gsfc.nasa.gov/>

³ <https://www.satimagingcorp.com/satellite-sensors/other-satellite-sensors/aster/>

⁴ <https://www.eumetsat.int/website/home/index.html>

⁵ <https://landsat.gsfc.nasa.gov/>

The rest of the paper is structured as follows. Section II gives related work. Sections III and IV describe data used in the paper and its preprocessing, respectively. Application of machine learning algorithms for crop classification is described in Section V and evaluated in Section VI. Finally, Section VII gives conclusion and future work.

II. RELATED WORK

There is a great amount of work done on land usage detection from satellite images, where R. Khatami et al. [6] gives some general guidelines, and C. Gomez et al. [7] provides challenges and opportunities. J. Fan et al. [13] use a single high-resolution image and apply pixel-based analysis to detect vegetation. Analysis is performed in two stages, firstly with supervised and secondly with unsupervised clustering. G. Alp et al. [14] take it further by classifying land usage based on CORINE nomenclature. While these methodologies prove to be beneficial for high level land usage classification, none of them address the challenge of crop classification.

N. Minallah et al. [15] try to distinguish 7 classes, out of which two are different type of crops. They achieve F-score of 0.88 using random forest. However, the score is achieved using 10-fold cross validation on the same data, without independent dataset for the evaluation. N. Laban et al. [10] achieve F-score of 0.89 using deep learning convolutional neural networks. They use separate evaluation dataset with prior geometric and radiometric corrections. However, out of 8 classes, two are crop types, namely sugar beet and wheat, which achieve individual recall of 0.64 and 0.88, and precision of 0.03 and 0.52, respectively. Another use of convolutional neural networks is presented by N. Kussul et al. [8] where overall accuracy of 0.85 is achieved on multiple crop types. A supervised decision tree classification is used by C. Boryan et al. [16] representing an initial work done by NASS, which database is used as the ground truth in our work.

Following publications use additional expert data to improve accuracy, namely phenological patterns. In [12], this pattern is extracted from NDVI index, Jeffries-Matusita Distance is used for data aggregation, while random forest is used as a classifier on multi-temporal images. Their overall accuracy is 0.91 with 4 crop types. R. Luciani et al. [11] include additional expert knowledge in form of prior knowledge of the area. They classify maize and two season wheat with decision tree approach and achieve overall accuracy of 0.93. Other approaches use prior knowledge of parcel boundaries to improve pixel-based classification as in [9]. However, these approaches require model driven approaches and thus limit the scalability and generality of the approach.

III. DATA SOURCES

Characteristics of satellite images are defined by four resolution types, namely spatial, spectral, temporal and radiometric resolution [2].

- **Spatial resolution** shows how many details there are in every image pixel. If a sensor has a spatial resolution of 10 meters, every pixel of an image obtained from that sensor covers ground area of 10m x 10m.
- **Spectral resolution** refers to the amount of spectral details in a band and is represented by the number of spectral bands in which the sensor collects data. Sensors with high spectral resolution have more narrow bands and those with low spectral resolution have broader bands where each band covers more of the spectrum.

- **Temporal resolution** represents how often the satellite revisits the observed object or phenomenon. If the satellite passes an area of interest every 5 days, the temporal resolution is every 5 days.
- **Radiometric resolution** is the ability to distinguish small differences in electromagnetic energy. In satellite imagery this is represented by how much information each pixel contains and is indicated by units of bits.

A. Input data

Data source used in this paper are Sentinel-2A and Sentinel-2B satellites, one of the seven missions currently in development under the Sentinel programme. The Sentinel programme is a group of missions providing data in the Copernicus programme, European Union's Earth Observation Programme, coordinated and managed by the European Commission in partnership with the Member States and various other EU organizations [18]. Sentinel-2A and Sentinel-2B were launched on June 22 2015 and on March 7 2017, respectively, and since then they have been flying in the same orbit but phased at 180°. Data used in our work is downloaded from the Sentinel Hub online service operated by Sinergise Ltd. [19], that provides modified and preprocessed Copernicus Sentinel data.

TABLE I. SPECTRAL BANDS OF SENTINEL-2 SATELLITES

<i>Band name</i>	<i>Resolution (m per pixel)</i>	<i>Wavelength (nm)</i>	<i>Bandwidth (nm)</i>	<i>Purpose</i>
B01	60	443	20	Aerosol detection
B02 (Blue)	10	490	65	Blue
B03 (Green)	10	560	35	Green
B04 (Red)	10	665	30	Red
B05 (Red edge)	20	705	15	Classifying the vegetation
B06	20	740	15	Classifying the vegetation
B07	20	783	20	Classifying the vegetation
B08A	20	865	20	Classifying the vegetation
B08 – NIR (Near Infra-red)	10	842	115	Near infrared
B09	60	945	20	Detecting the water vapour
B10	60	1375	30	Cirrus cloud detection
B11	20	1610	90	Snow/ice/cloud discrimination
B12 – SWIR (Short-wave Infra-red)	20	2190	180	Snow/ice/cloud discrimination

Sentinel-2 has three possible spatial resolutions and several spectral resolutions, i.e., bandwidths, with radiometric resolution of 12 bits, which means that $2^{12}=4096$ different values can be distinguished, and finally with temporal resolution of 5 days. Table I shows a list of 13 different spectral bands from Sentinel-2 with their main characteristics. The bands are used for calculating 15 standard indices listed in Table II [5], which are used throughout the paper as multi-spectral data for crop classification. Moreover, spatial resolution of 29m x 36m is used in order to match the resolution with the evaluation data.

TABLE II. INDICES AND THEIR FORMULATION⁶

Name	Formula
ARI	$\frac{1.0}{B03} - \frac{1.0}{B05}$
ARVI	$\frac{B09 - B04 - \gamma * (B04 - B02)}{B09 + B04 - \gamma * (B04 - B02)}$
CHL-RED-EDGE	$\frac{B07^{-1}}{B05}$
EVI	$2.5 * \frac{B08 - B04}{B08 + 6 * B04 - 7.5 * B02 + 1}$
EVI2	$2.4 * \frac{B08 - B04}{B08 + B04 + 1.0}$
GNDVI	$\frac{B08 - B03}{B08 + B03}$
MCARI	$((B05 - B04) - 0.2 * (B05 - B03)) * \frac{B05}{B04}$
MSI	$\frac{B11}{B08}$
NBR	$\frac{B08 - B12}{B08 + B12}$
NDII	$\frac{B08 - B11}{B08 + B11}$
NDVI	$\frac{B08 - B04}{B08 + B04}$
NDWI	$\frac{B03 - B08}{B03 + B08}$
PSSR	$\frac{B08}{B04}$
SAVI	$\frac{B08 - B04}{B08 + B04 + L} * (1.0 + L)$
SIPI	$\frac{B08 - B01}{B08 - B04}$

B. Evaluation data

The data used for the evaluation is provided by National Agricultural Statistics Service (NASS) by United States Department of Agriculture [17]. The data is formatted as Cropland Data Layer (CDL), i.e., geospatial data. The CDL is a raster, geo-referenced, crop-specific land cover data layer created annually for the continental United States using moderate resolution satellite imagery and extensive agricultural ground truth. However, CDL data accuracy varies between different crops and states in the US, thus only crops with high accuracy scores are chosen as training and evaluation data. Otherwise, the evaluation would be performed against the faulty data, thus rendering the results unusable.

IV. METHODOLOGY

This section describes the process of acquiring and preprocessing the satellite images prior the analysis. Firstly, a sequence of satellite images over a period of one year is downloaded for several areas in US. Secondly, the images with high cloud coverage are removed from the dataset as are not usable for analysis. Thirdly, the remaining images (24 to 37 images, depending on a geographical area) for each area are aggregated separately by averaging the pixel values on a temporal axis. The result is a set of images, one for each selected area in US, containing the annual average values of the index at each pixel. The same procedure is repeated for each index, as depicted in Fig. 1.

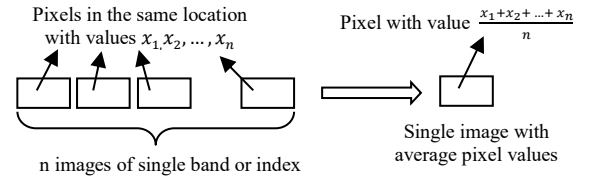


Fig. 1. Preprocessing of satellite images for single index

Ground truth data from CDL is obtained for the same selected areas for the specified year. However, since the accuracy of CDL data depends on the crop type and geographical location, as mentioned in the previous section, only areas containing high accuracy crops are analyzed. Table III contains a list of selected crops with their respective accuracy scores in California, US. Recall represents a proportion of actual positives that are identified correctly, precision is a proportion of positive identification that are actually correct, while Kappa is a combination of those two.

TABLE III. SELECTED CROPS FROM CDL DATABASE WITH THEIR RESPECTIVE ACCURACY SCORES IN CALIFORNIA, US

Crop type	Recall	Precision	Kappa
Rice	0.974	0.987	0.972
Grapes	0.983	0.983	0.983
Almonds	0.932	0.972	0.927
Walnuts	0.942	0.961	0.941
Pistachios	0.937	0.991	0.934
Avocado	0.999	0.969	0.999
Pomegranates	0.931	0.959	0.931

The images are transformed into the table format where every row represents a pixel with its corresponding average values of all indices and CDL class. An excerpt from the table is presented in Table IV. The rows are then further filtered to include only those that correspond to a list of selected crops, as only those crops can be correctly trained and evaluated. Such datasets are used both for building a crop classification models using machine learning, as well as validating those models.

TABLE IV. EXCERPT FROM THE DATASET

ARI*	EVI*	NDVI*	NDWI*	... **	CDL class
1.63287	0.13674	0.25313	-0.29978	...	Avocado
1.16493	0.23225	0.2702	-0.33484	...	Grapes

* Indices values are average values over a period of one year

** Three dots represent 11 other indices

To avoid biased learning, as well as biased interpretation of results, the dataset is stratified so that each crop type holds the same number of pixels during the analysis. This way, machine learning algorithms will not overfit or prefer a single crop type, while during the validation the overall results will not be highly influenced by the success or failure of a single crop type classification.

V. CROP CLASSIFICATION WITH MACHINE LEARNING

Machine learning models are trained on a dataset taken from the six areas in California during 2018, as depicted in Fig. 2. The areas are selected arbitrarily to include all crops listed in Table III, with each crop holding 28,550 pixels after stratification, which is a total of 199,850 pixels used as a training dataset. The dataset is then divided into 10 equal segments used to perform 10-fold cross validation.

⁶ https://sentinel-hub.com/develop/documentation/eo_products/Sentinel2EOproducts

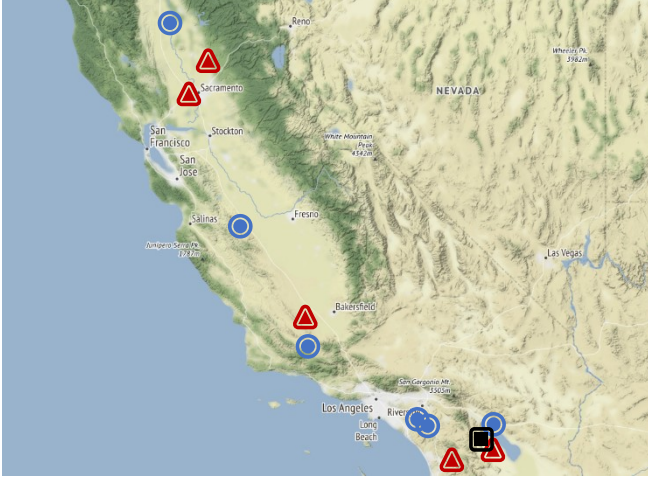


Fig. 2. Areas in California used as training (blue circles) and evaluation (red triangles) datasets, as well as one used in the discussion (black rectangle)

Total of 12 classification models are built and compared. In order to encompass linear, non-linear and tree-based classification models, several representative models of each of the categories are evaluated, namely linear discriminant analysis, penalized discriminant analysis and linear-based support vector machines as linear models; k-nearest neighbors and neural network as nonlinear models and random forest as tree-based model. For random forest, k-nearest neighbors and neural network model tuning is performed. All classification models along with their parameters and performance results are listed in Table V.

TABLE V. PERFORMANCE OF MACHINE LEARNING MODELS

<i>Models</i>	<i>Accuracy</i>	<i>Kappa</i>
Linear discriminant analysis	0.7209057	0.6743900
Penalized discriminant analysis	0.7209007	0.6743841
Random forest (mtry=2)	0.9036928	0.8876416
Random forest (mtry=8)*	0.9046185	0.8887215
Random forest (mtry=15)	0.8963673	0.8790952
K-nearest neighbors (k=5)	0.8926145	0.8747169
K-nearest neighbors (k=7)	0.8895372	0.8711267
K-nearest neighbors (k=9)	0.8859945	0.8669936
Support vector machines (linear)	0.7937203	0.7593403
Neural network (size=4, decay=0.01)	0.7307631	0.6858903
Neural network (size=4, decay=0.1)	0.7193195	0.6725394
Neural network (size=8, decay=0.01)	0.7765074	0.7392586

* Random forest achieves best results

Among evaluated models, random forest and K-nearest neighbors show best results. The highest accuracy of 0.9046 is achieved for random forest model with mtry=8, representing a parameter that defines number of variables for splitting at each tree node.

VI. EVALUATION AND DISCUSSION

Methodology proposed in this paper, along with the random forest model built in the previous section that exhibited the highest accuracy is evaluated with a separate dataset. The dataset is created from 5 new areas in California depicted in Fig. 2 containing again all 7 crop types. After stratification the evaluation dataset holds total of 13,349 pixels, that is 1,907 pixels per crop type.

A. Validation

Overall accuracy of the random forest model applied on the evaluation dataset is **0.842**, with Kappa score being **0.815**. More detailed results are shown in Table IV in a form of normalized confusion matrix containing 7 crop types, while Table VII holds the precision and recall scores of the random forest predictions for each crop separately.

TABLE VI. NORMALIZED CONFUSION MATRIX FOR RANDOM FOREST

<i>Original</i>	<i>Predicted</i>						
	<i>Rice</i>	<i>Grapes</i>	<i>Almonds</i>	<i>Walnuts</i>	<i>Pistachios</i>	<i>Avocados</i>	<i>Pomegranates</i>
<i>Rice</i>	0.898	0.014	0.016	0.009	0.006	0.019	0.038
<i>Grapes</i>	0.002	0.955	0.005	0.002	0.014	0.002	0.019
<i>Almonds</i>	0.003	0.045	0.855	0.008	0.03	0.016	0.043
<i>Walnuts</i>	0.003	0.09	0.104	0.698	0.009	0.075	0.021
<i>Pistachios</i>	0.002	0.228	0.015	0.073	0.578	0.018	0.086
<i>Avocados</i>	0	0.001	0.001	0.001	0	0.997	0.001
<i>Pomegranates</i>	0	0.048	0.008	0.007	0.022	0.002	0.913

Classification of avocados and grapes exhibit excellent results, namely 0.997 and 0.946, respectively. However, pistachios and walnuts do not perform very well, where former achieves recall of only 0.596 with 0.239 being classified as grapes, while latter gets scattered over almonds, avocados and grapes, thus achieving recall of only 0.681. Nevertheless, all the crop types except grapes achieve precision above 0.81, implying that most of the predicted crops are of that type. However, in order to reason the misclassification of pistachios with grapes, further analysis is performed and discussed in the following subsection.

TABLE VII. RECALL AND PRECISION OF RANDOM FOREST MODEL FOR EACH CROP TYPE

<i>Crop type</i>	<i>Recall</i>	<i>Precision</i>
Rice	0.9093	0.9890
Grapes	0.9460	0.6925
Almonds	0.8547	0.8512
Walnuts	0.6812	0.8740
Pistachios	0.5957	0.8767
Avocado	0.9969	0.8821
Pomegranates	0.9124	0.8151

B. Discussion

Table VI clearly shows that grapes take precedence over pistachios, as well as walnuts and almonds, where general precedence of grapes is visible from its precision score of 0.6925 in Table VII. Therefore, an additional agricultural area in California containing grapes is examined closely. The location of the area is depicted in Fig. 2, and it contains 980 pixels of grapes. Unlike in the previous subsection, no stratification is performed in order to retain the entire image, while only pixels containing selected crops from Table VII are taken. A single image of the area from April 11th 2018 is depicted in Fig. 3a, along with the CDL image (Fig. 3b), random forest classification (Fig. 3c) and the difference between CDL and random forest classification (Fig. 3d).

Fields in the top left corner of Fig. 3c are classified as pistachios by the random forest model, while they are classified as grapes by CDL (Fig. 3b). Observing the sequence of true color images, the mentioned fields do not resemble other fields of grapes, which is also visible in Fig. 3a. Similarly, straight vertical lines visible in Fig. 3c on the left-hand side fields represent walkways between fields and crops, and are detected by the random forest model, while CDL classifies them as grapes. Furthermore, field in the right bottom corner of Fig. 3b shows CDL classification of grapes, while random forest (Fig. 3c) shows some scattered non-grape pixels. By observing a sequence of images throughout 2018 it is evident that the mentioned scattered pixels represent decay of grapes, which is also seen in Fig. 3a.

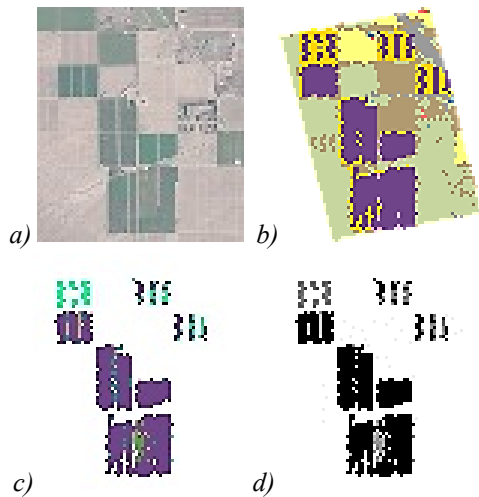


Fig. 3. Comparison between the results and ground truth: a) original satellite image, b) CDL from NASS, c) Random forest classification, d) Difference between random forest and CDL (black pixels represent the same, while gray pixels represents different classification)

Above examples imply that CDL overclassifies grapes. Since our model uses this data for learning, the resulting model also gives precedence to grapes as it learns from the data that classifies much broader combination of inputs as grapes, which are false positives. However, due to clear distinction between grape pixels and something else, the model still tries to classify them as something else. Consequently, it is forced to classify them as one of the other 6 crops. Example are pixels in the upper right corner, which are classified as grapes by CDL and thus are part of the validation dataset, while they should be excluded. This could be avoided with a high-level classification that would eliminate water, urban area and other non-agriculture classes so that prediction could be done only on agriculture pixels.

VII. CONCLUSION AND FUTURE WORK

In this paper, we have applied several machine learning algorithms on multi-spectral and multi-temporal satellite images, and successfully classified 7 different crop types with the accuracy score of 0.8420. This way, we demonstrated that satellite images can be used for crop classification with satisfying accuracy, minimum image preprocessing and no agricultural domain knowledge. Additionally, by classifying only crop types we achieved better resolution, which provided improved results per crops compared to the related work.

For our future work, we plan to apply machine learning algorithms directly on raw bands without calculating indices, as well as include location-awareness in our model training that will exploit similarity of neighboring pixels with higher number of crop types. This will give us more universal data-driven crop classification models. Finally, we plan to acquire

better ground truth data that will have higher accuracy score to avoid false modeling during the learning and validation phase.

REFERENCES

- [1] Navalgund, Ranganath & V, Jayaraman & Roy, Parth. (2007). *Remotesensing applications: An overview*. Currentscience. Vol. 93.
- [2] Campbell, J. B. "Introduction to Remote Sensing". New York London: The Guilford Press, 2002
- [3] G. James, D. Witten, T. Hastie, and R. Tibshirani. "An Introduction to Statistical Learning: With Applications in R". Springer Publishing Company, Incorporated. 2014
- [4] W. Qihao, "Introduction to Remote Sensing Systems, Data, and Applications", 2013. doi: 10.1201/b15159-3.
- [5] Jinru, Xue & Su, Baofeng. (2017). "Significant Remote Sensing Vegetation Indices: A Review of Developments and Applications." *Journal of Sensors*. 2017. 1-17. doi: 10.1155/2017/1353691.
- [6] R. Khatami, G. Mountrakis, and S. V. Stehman, "A meta-analysis of remote sensing research on supervised pixel-based land-cover image classification processes: General guidelines for practitioners and future research," *Remote Sensing of Environment*, vol. 177, pp. 89 – 100, 2016. doi: 10.1016/j.rse.2016.02.028
- [7] C. Gómez, J.C. White and M.A. Wulderl, "Optical remotely sensed time series data for land cover classification: A review", *ISPRS Journal of Photogrammetry and Remote Sensing*, Vol. 116, pp.55–72, 2016. doi: 10.1016/j.isprsjprs.2016.03.008
- [8] N. Kussul, M. Lavreniuk, S. Skakun and A. Shelestov, "Deep Learning Classification of Land Cover and Crop Types Using Remote Sensing Data," in *IEEE Geoscience and Remote Sensing Letters*, vol. 14, no. 5, pp. 778-782, May 2017. doi: 10.1109/LGRS.2017.2681128
- [9] N. Kussul, G. Lemoine, F. J. Gallego, S. V. Skakun, M. Lavreniuk and A. Y. Shelestov, "Parcel-Based Crop Classification in Ukraine Using Landsat-8 Data and Sentinel-1A Data," in *IEEE Journal of Selected Topics in Applied Earth Observations and Remote Sensing*, vol. 9, no. 6, pp. 2500-2508, June 2016. doi: 10.1109/JSTARS.2016.2560141
- [10] N. Laban, B. Abdellatif, H. M. Ebeid, H. A. Shedeed and M. F. Tolba, "Seasonal Multi-temporal Pixel Based Crop Types and Land Cover Classification for Satellite Images using Convolutional Neural Networks," 2018 13th International Conference on Computer Engineering and Systems (ICCES), Cairo, Egypt, 2018, pp. 21-26. doi: 10.1109/ICCES.2018.8639232
- [11] R. Luciani, G. Laneve, M. Jahjah and M. Collins, "Crop species classification: A phenology based approach," 2017 IEEE International Geoscience and Remote Sensing Symposium (IGARSS), Fort Worth, TX, 2017, pp. 4390-4393. doi: 10.1109/IGARSS.2017.8127974
- [12] A. Khaliq, L. Peroni and M. Chiaberge, "Land cover and crop classification using multitemporal sentinel-2 images based on crops phenological cycle," 2018 IEEE Workshop on Environmental, Energy, and Structural Monitoring Systems (EESMS), Salerno, 2018, pp. 1-5. doi: 10.1109/EESMS.2018.8405830
- [13] J. Fan, T. Chen and S. Lu, "Vegetation coverage detection from very high resolution satellite imagery," 2015 Visual Communications and Image Processing (VCIP), Singapore, 2015, pp. 1-4. doi: 10.1109/VCIP.2015.7457846
- [14] G. Alp, I. Y. Algan and E. Sertel, "Determination of agricultural land changes in Mugla, Turkey using remotely sensed data and Corine methodology," 2015 Fourth International Conference on Agro-Geoinformatics (Agro-geoinformatics), Istanbul, 2015, pp. 7-10. doi: 10.1109/Agro-Geoinformatics.2015.7248083
- [15] N. Minallah, H. Ur Rahman, R. Khan, A. Alkhalifah and S. Khan, "Land usage analysis: A random forest approach," 2015 7th International Conference on Recent Advances in Space Technologies (RAST), Istanbul, 2015, pp. 245-249. doi: 10.1109/RAST.2015.7208349
- [16] C. Boryan, Z. Yang, R. Mueller, M. Craig, Monitoring US agriculture: The US Department of Agriculture, National Agricultural Statistics Service, Cropland Data Layer Program. Geocarto International. 2011, 26. 341-358. 10.1080/10106049.2011.562309.
- [17] United States Department of Agriculture (USDA), National Agricultural Statistics Service (NASS), "2018 California Cropland Data Layer", 2018 Edition, USDA, NASS Marketing and Information Services Office, Washington, D.C., 2018.
- [18] "Copernicus: The EU Earth Observation and Monitoring", Copernicus Programme, <https://www.copernicus.eu>, European Commission
- [19] "Modified Copernicus Sentinel data 2019/Sentinel Hub", Sentinel Hub, <https://sentinel-hub.com/>, Sinergise Lt